Int. J. Production Economics 262 (2023) 108928

Contents lists available at ScienceDirect

International Journal of Production Economics

journal homepage: www.elsevier.com/locate/ijpe

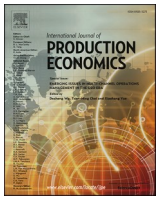

Modelling and optimisation of energy consumption and profit-oriented multi-parallel partial disassembly line balancing problem

Wei Liang [a,b], Zeqiang Zhang [a,b,*,1], Tao Yin [a,b], Yu Zhang [a,b], Tengfei Wu [a,b]

[a] School of Mechanical Engineering, Southwest Jiaotong University, 610031, Chengdu, China
[b] Technology and Equipment of Rail Transit Operation and Maintenance Key Laboratory of Sichuan Province, 610031, Chengdu, China

ARTICLE INFO

Keywords:
Multi-parallel line layout
Partial disassembly mode
Exact solution
Genetic and tabu search algorithm
Hybrid products

ABSTRACT

Based on the actual requirements of recycling enterprises, this study proposes a multi-parallel partial disassembly line balancing problem (MPPDLBP). Four objectives, the number of shared workstations, workstation load balancing index, energy consumption, and profit, need to be optimised in MPPDLBP. To address the MPPDLBP, this study further constructs a mixed-integer nonlinear programming (MINLP) model and designs a suitable mechanism of encoding and decoding. Meanwhile, partial disassembly is adopted in this study because recycling enterprises aim for low energy consumption and high profits. In addition, the positions of the best values for each objective are defined as the best disassembly levels. Furthermore, this study proposes a genetic and tabu search algorithm (GATS) for optimising the MPPDLBP effectively. The superior performance of the proposed GATS is verified by comparing it with other effective algorithms in existing literature. Finally, this study optimises a hybrid instance and provides decision-makers with multiple low-energy and high-profit disassembly schemes.

1. Introduction

At present, productions are closely related to the environment and economy (Battaïa and Dolgui, 2013). Due to environmental deterioration, the green and recycling economy has become a theme of industry. However, many reusable resources are wasteful because of the unreasonable disposal of waste products. Even hazardous chemicals have polluted the environment with waste products, such as lead, cadmium, and mercury. Therefore, resource recovery is essential to ensuring environmental friendliness and a recycling economy (Battaïa and Dolgui, 2022). Disassembly is an important step toward resource recovery. Before standardized disassembly lines were adopted by recycling enterprises, individuals disassembled most of the waste products in small workshops. But small workshops are not only inefficient but also polluting the environment. Furthermore, recycling through disassembly lines is more standardized and efficient than conventional methods such as small workshop operation (Hasegawa et al., 2019).

Although many resource-recycling enterprises have widely employed disassembly lines, they still have many problems that need to be solved. First, the ultimate goal of enterprises is to reduce the disassembly cost and thus gain greater profitability (Godichaud and Amodeo, 2018). Second, environmental policies impose many restrictions on disassembly enterprises, such as hazardous parts must be removed. In addition, enterprises should consider balancing the workload of employees tasked with dismantling and maximising the conversion of benefits when designing disassembly schemes. Thus, the disassembly line balancing problem (DLBP) is a crucial topic in the recycling industry (Diri Kenger, Koç, and Özceylan, 2021). Moreover, various waste products separated by multi-parallel disassembly lines, as shown in Fig. 1, is already familiar in resource-recycling enterprises. Meanwhile, most recycling enterprises adopted the partial disassembly mode to maximise profits. Therefore, providing resource-recycling enterprises with suitable disassembly schemes in partial disassembly mode based on the multi-parallel line layout is desirable.

The main contributions of this study are as follows:

- This study proposes a multi-parallel partial disassembly line balancing problem (MPPDLBP) based on the requirements of resource-recycling enterprises.
- This study constructs a mixed-integer nonlinear programming (MINLP) model, which can be applied to solve four objectives: the number of shared workstations, workstation load balancing index, energy consumption, and profit.

* Corresponding author.School of Mechanical Engineering, Southwest Jiaotong University, 610031, Chengdu, China.
E-mail addresses: liangwei@my.swjtu.edu.cn (W. Liang), zhangzq@home.swjtu.edu.cn (Z. Zhang), amniyim@my.swjtu.edu.cn (T. Yin), chaizhong1997@gmail.com (Y. Zhang), wtenfi@gmail.com (T. Wu).
[1] Postal address: School of Mechanical Engineering, Southwest Jiaotong University, Chengdu, 610031, China.

https://doi.org/10.1016/j.ijpe.2023.108928
Received 28 April 2022; Received in revised form 21 April 2023; Accepted 19 May 2023
Available online 20 May 2023

Parameters description

i, j	Task indexes
a, b, c	Number of tasks of each parallel line
n	Maximum number of tasks on all parallel lines. $n = \max\{a, b, c\}$
$\boldsymbol{I}$	Set of tasks for the maximum number of tasks. $\boldsymbol{I} = \{1, 2, \ldots, n\}$
$\boldsymbol{L}$	Set of parallel line indexes. $\boldsymbol{L} = \{1, 2, 3\}$
l, u	Parallel line indexes
$\boldsymbol{R}$	Set of workstation column indexes. $\boldsymbol{R} = \{1, 2\}$
r	Workstation column index
m	Maximum number of available shared workstations
$\boldsymbol{M}$	Set of shared workstations. $\boldsymbol{M} = \{1, 2, \ldots, m\}$
k	Shared workstation index. $k \in \boldsymbol{M}$
$\boldsymbol{O}$	Set of disassembly order indexes for tasks. $\boldsymbol{O} = \{1, 2, \ldots, m\}$
o	Disassembly order index for tasks. $o \in \boldsymbol{O}$
CT	Cycle time
t_i^l	Operation time for task i on the parallel line l
$\boldsymbol{TP}_{ij}^l$	Precedence relationship matrix. For waste products on parallel line l, if task i is a predecessor task of task j, $\boldsymbol{TP}_{ij}^l = 1$; Otherwise, $\boldsymbol{TP}_{ij}^l = 0$
α	A large number
h_i^l	Hazardous attribute. If task i on the parallel line l is hazardous, $h_i^l = 1$; Otherwise, $h_i^l = 0$
d_i^l	Demand attribute. If task i on the parallel line l is in-demand, $d_i^l = 1$; Otherwise, $d_i^l = 0$
ew	Unit time energy consumption of an activated shared workstation
el	Unit time energy consumption of auxiliary equipment
eh	Extra unit time energy consumption for disassembling hazardous parts
ed	Extra unit time energy consumption for disassembling in-demand parts
cw	Unit time cost for an activated shared workstation
ch	Extra unit time cost for disassembling hazardous parts
cd	Extra unit time cost for disassembling in-demand parts
f_i^l	Profit of task i on the parallel line l
WT	Number of shared workstations
TB	Workstation load balancing index
EC	Energy consumption
PF	Total profit
Variables	
w_i^l	Start time for task i on the parallel line l being disassembled
x_{iko}^{lr}	Assignment variable for tasks. If task i on the parallel line l is disassembled at order index o of the shared workstation k in column r, $x_{iko}^{lr} = 1$; Otherwise, $x_{iko}^{lr} = 0$
$S\ r\ k$	Activation variable for shared workstations. If shared workstation k in column r is activated, $S_k^r = 1$; Otherwise, $S\ r\ k = 0$

Fig. 1. A layout of multi-parallel disassembly lines.

- This study designs a mechanism of encoding and decoding and proposes a genetic and tabu search algorithm (GATS) according to the characteristics of the MPPDLBP.

The remainder of this paper is organised as follows. Section 2 analyses the relevant studies of DLBP. Section 3 describes the MPPDLBP and constructs a MINLP model. Section 4 explains the proposed GATS and the encoding and decoding mechanisms in detail. Section 5 validates the MINLP model and GATS by solving several instances. Meanwhile, the performance of GATS is compared with four algorithms in Section 5. Section 6 optimises an instance containing three kinds of waste products. Finally, Section 7 summarises this study and prospects the future researches of DLBP.

2. Study analysis

The DLBP (Gupta and Gungor, 2001) has been studied extensively. This section focuses on the relevant studies of the DLBP in terms of disassembly layouts, disassembly levels, optimisation objectives, and solution methods. The characteristics of the relevant studies are summarised in Table 1.

2.1. Disassembly layouts

The straight layout is one of the most studied layouts. Kalayci and Gupta (2013), Bentaha et al. (2020), and Kucukkoc et al. (2020b) have investigated straight layout in several requirements. For two-sided and U-shaped layouts with different application environments, some researchers have also focused on them. Zhang et al. (2022) modelled and optimised the two-sided layout considering the part features. Li and Janardhanan (2021) investigated the U-shaped layout for maximising profit. In addition, as recycling enterprises showed a growing preference for parallel layout, studies of parallel layout are increasingly popular. For example, Zhu et al., 2020 and Liang et al. (2023a,b) published studies on parallel layout in recent years. However, all existing studies focused on the parallel layout involving two parallel lines. Moreover, the existing methods cannot solve the parallel layout problem with more than two parallel lines. Therefore, the parallel layout with more than two parallel lines needs to be further investigated.

2.2. Disassembly levels

The studies on disassembly levels of the DLBP mainly include complete (McGovern and Gupta, 2006; Zhu et al., 2018; Ren et al., 2020) and partial disassembly modes (Yin et al., 2021; Xia et al., 2020). The number of parts disassembled from a waste product varies in different disassembly modes. The complete disassembly mode means that all parts of a waste product must be separated, whereas the partial disassembly mode indicates that the parts are removed selectively. For example, Zhu et al. (2018) studied the disassembly schemes for a waste refrigerator case containing twenty-five tasks in a complete disassembly mode, i.e., all twenty-five components were removed. On the other hand, Yin et al. (2021) investigated the disassembly schemes for a waste laptop case containing forty-seven components in a partial disassembly mode. A study by Yin et al. showed that hazardous components could be successfully removed from a waste laptop by disassembling forty-two

Table 1
Characteristics of relevant studies.

Literature	Layouts					Levels		Objectives					Methods	
	S	T	U	P	MP	C	PT	F_1	F_2	F_3	F_4	F_5	IA	EM
McGovern et al. (2006)	✓					✓		*WT*	*TB*	*HI*	*DI*	*DC*	✓	
Zhu et al. (2018)	✓					✓		*WT*	*SR*	*HI*			✓	
Ren et al. (2020)	✓					✓		*WT*	*TB*	*HI*	*DI*	*WT*	✓	
Yin et al. (2021)	✓						✓	*WT*	*TT*	*TB*	*NT*		✓	
Xia et al. (2020)	✓						✓	*WT*	*TB*	*DI*	*CS*		✓	
Bentaha et al. (2020)	✓						✓	*PF*						✓
Li and Janardhanan (2021)			✓				✓	*PF*					✓	✓
Wang et al. (2020)			✓			✓		*WT*	*TB*	*EC*	*PF*		✓	
Ren et al. (2017)	✓						✓	*PF*					✓	✓
Edis et al. (2022)	✓						✓	*PF*						✓
Bentaha et al. (2018)	✓						✓	*PF*						✓
Bentaha et al. (2015)	✓					✓		*CS*						✓
Pour-Massahian-Tafti et al. (2021)	✓					✓		*CS*						✓
Bentaha et al. (2014)	✓					✓		*CS*						✓
Zou et al. (2018)	✓					✓		*SI*	*NT*	*CS*			✓	
Wang et al. (2022)	✓						✓	*WT*	*PF*	*EC*	*TB*		✓	
Kucukkoc et al. (2020)	✓					✓		*WT*	*CT*					✓
He et al. (2022)	✓					✓		*CS*						✓
Zhang et al. (2022)		✓				✓		*WT*	*TB*	*HI*	*DI*		✓	✓
Edis et al. (2019)	✓					✓		*TB*	*DI*	*HI*	*DC*			✓
Zhang et al. (2017)	✓					✓		*WT*	*TB*	*CS*	*DC*		✓	✓
Go et al. (2012)	✓					✓		*TT*					✓	
Kucukkoc (2020)		✓				✓		*WT*					✓	✓
Kalayci and Gupta (2013)	✓					✓		*TB*	*HI*	*DI*			✓	
Liang et al. (2023)	✓							*WT*	*TB*	*NT*	*EC*		✓	✓
Zhu et al. (2020a)				✓			✓	*CT*	*WT*	*TB*	*NT*		✓	
This study					✓		✓	*WT*	*TB*	*EC*	*PF*		✓	✓

**S*: straight; *T*: two-sided; *U*: U-shape; *P*: parallel; *MP*: multi-parallel; *C*: complete disassembly; *PT*: partial disassembly; *IA*: intelligent algorithm; *EM*: exact algorithm and exact model; *WT*: the number of workstations; *TB*: workstation load balancing index; *EC*: energy consumption; *PF*: profit; *HI*: hazard index; *DI*: demand index; *DC*: the number of direction changes required for disassembly; *SI*: smoothing index; *TT*: total disassembly time; *NT*: the number of disassembly tools; *CS*: cost; *CT*: cycle time.

components. The partial disassembly mode varies in disassembly levels (Bentaha et al., 2020), depending on the termination criteria of the disassembly. Presently, the best disassembly level for the partial disassembly mode is determined mainly through constraints: (1) hazardous tasks are completely removed; (2) Hazards and demand tasks are completely removed (Li and Janardhanan, 2021); and objective values: (1) the minimum energy consumption (Wang et al., 2020); (2) the minimum cost (Ren et al., 2017); (3) the maximum profit (Edis et al., 2022; Bentaha et al., 2018). Because of the superiorities of the partial disassembly mode, resource-recycling enterprises are more frequently adopting this model. To meet the requirements of recycling enterprises better, this study adopts two objective functions: minimum energy consumption and maximum profit as the performance criteria for the best disassembly level, while the hazardous tasks are completely disassembled.

2.3. Optimisation objectives

Various objectives, such as the disassembly cost (Bentaha et al., 2015; Pour-Massahian-Tafti et al., 2021; Bentaha et al., 2014), tool replacement times (Zou et al., 2018), change times of disassembly direction (Wang et al., 2022), and cycle time (*CT*) (Kucukkoc et al., 2020b), have been developed to evaluate the performance of the disassembly line. The number of workstations affects the area occupied by all demolition facilities. The fewer facilities a resource-recycling enterprise has, the less footprint it requires. Therefore, the number of workstations is one of the most frequently optimised indices in existing literature. For example, Ren et al. (2020), Wang et al. (2020), and Zhang et al. (2022) optimised the number of workstations under different layouts. Furthermore, the workstation load balancing index is a crucial objective for optimising the DLBP, which has been studied by Edis et al. (2019) and Xia et al. (2020). Moreover, recycling enterprises attach significant importance to energy consumption and profits. High profits promote the development of recycling enterprises, and low energy consumption will contribute to the elimination of environmental pollution. Thus, according to the characteristics of the DLBP and the requirements of recycling enterprises, four objectives, namely, the number of workstations, workstation load balancing index, energy consumption, and profit, are studied in this paper.

2.4. solution methods

Exact algorithms, intelligent algorithms, and exact models are the mainstream methods for solving the DLBP. The exact algorithm is an exact solution method that designs the algorithm structure according to the problems. For example, He et al. (2022) designed a sample average approximation algorithm and an L-shaped algorithm to solve a linear DLBP with an uncertain number of parts. However, exact algorithms are complex and challenging in solving large-scale cases. The exact model is way to obtain the optimal value by modelling the DLBP and solving it using exact optimisers such as GUROBI (Zhang et al., 2021), CPLEX (Edis et al., 2019), and LINGO (Zhang et al., 2017). Exact models can rapidly obtain optimal values of small-scale instances. However, because of the explosive growth of the problems solution space, the exact models cannot obtain the optimal values in a specific time when solving medium-scale and large-scale instances. For example, Kucukkoc (2020) tested several cases with different scales by using an exact model, showing that the exact model failed to obtain the optimal values in a limited time after the cases exceeded 25 in size. Furthermore, intelligent algorithms, such as the genetic algorithm (GA) (Go et al., 2012; Nahas et al., 2014; Kucukkoc, 2020), tabu search algorithm, particle swarm algorithm (Kalayci and Gupta, 2013), social spider algorithm (Liang et al., 2023), and artificial fish swarm algorithm (Z. Zhang et al., 2017), have been employed for solving the DLBP. Intelligent algorithms are distinguishable from exact solutions. Intelligent algorithms can continuously approach the optimal solution through iterations, but their

output solutions are only sometimes optimal. Intelligent algorithms have the advantage of obtaining solutions in a short time when solving medium-scale and large-scale instances. For example, Liang et al. (2023) obtained a set of feasible solutions within 79.58s for a large-scale case by employing an intelligent algorithm. Nevertheless, the effectiveness of the solution method cannot be validated while the problem is just solved by designed encoding and decoding mechanisms. Although exact models have no advantage in solving large-scale cases, they can be utilised to obtain the optimal solutions of small-scale cases, which can be taken as the comparison references for intelligent algorithms in solving the DLBP. Hence, both the exact model and intelligent algorithm are developed in this study.

3. Problem description

3.1. Problem statement

The multi-parallel disassembly line balancing problem (MPDLBP) refers to the balancing problem that involves more than two parallel disassembly lines. This study defines the MPPDLBP as a problem involving three parallel lines and employing the partial disassembly mode according to the surveys of recycling enterprises. Furthermore, MPPDLBP optimises four objectives: the number of workstations, workstation load balancing index, energy consumption, and profit. The layout of the MPPDLBP optimised in this study containing three parallel lines and two columns of shared workstations is shown in Fig. 2. The three lines are arranged in parallel, and the two columns of shared workstations are positioned between the parallel lines. Then, each shared workstation is responsible for disposing of tasks from both sides of shared workstations.

The complete disassembly mode takes longer processing time and may consume more energy than the partial disassembly mode. Smith et al. (2016) studied the relationship between the profit and processing time. The relationship between the profit and cost versus disassembly time is shown in Fig. 3. As depicted in Fig. 3, both gross receipts and costs trend upward over time, profit peaks at some time and then trends downward. Therefore, terminating disassembly at a peak profit by employing the partial disassembly mode is a practical design. In addition, the government requires that all hazardous parts must be removed because hazardous parts may contaminate the environment owing to hazardous chemicals. Thus, this study aims to maximise the profit and minimise the number of shared workstations, workstation load balancing index, and energy consumption under the premise that all hazardous parts are separated.

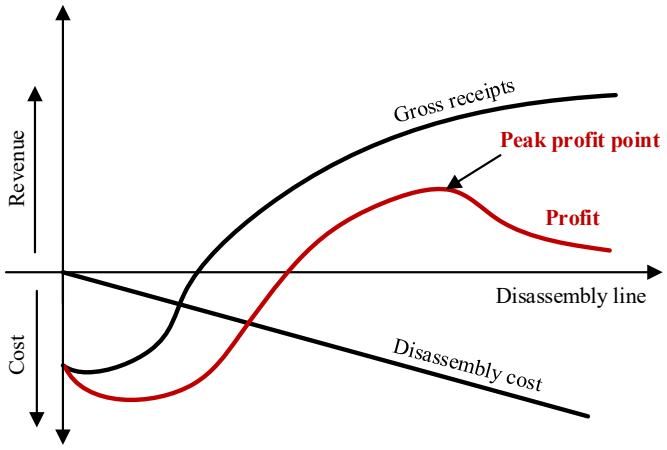

Fig. 3. Relationship between disassembly economics and disassembly time.

3.2. MINLP model construction

The constraints of models in the existing literature on solving partial disassembly mode have non-linear constraints (Yin et al., 2022). However, the non-linear constraints will increase the solution complexity dramatically. Therefore, a model without non-linear constraint is developed in this study.

Objective functions

$$WT = \min \sum_{r=1}^{\|\boldsymbol{R}\|} \sum_{k=1}^{m} S_k^r \tag{1}$$

$$TB = \min \sum_{r=1}^{\|\boldsymbol{R}\|} \sum_{k=1}^{m} \left(S_k^r \cdot CT - \sum_{l \in \{\boldsymbol{L} | r+1 \geq l \geq r\}} \sum_{i=1}^{n} \sum_{o=1}^{\|\boldsymbol{O}\|} \left(x_{iko}^{lr} \cdot t_i^l \right) \right)^2 \tag{2}$$

$$EC = \min \left(\sum_{r=1}^{\|\boldsymbol{R}\|} \sum_{k=1}^{m} S_k^r \cdot CT \cdot (ew + el) + \sum_{l=1}^{\|\boldsymbol{L}\|} \sum_{i=1}^{n} \left(h_i^l \cdot t_i^l \right) \cdot eh + \sum_{l=1}^{\|\boldsymbol{L}\|} \times \sum_{i=1}^{n} \left(\sum_{r \in \{\boldsymbol{R} | r+1 \geq l \geq r\}} \sum_{k=1}^{m} \sum_{o=1}^{\|\boldsymbol{O}\|} x_{iko}^{lr} \cdot d_i^l \cdot t_i^l \right) \cdot ed \right) \tag{3}$$

Eq. (1) minimises the number of shared workstations. Eq. (2) minimises the workstation load balancing index, which balances the

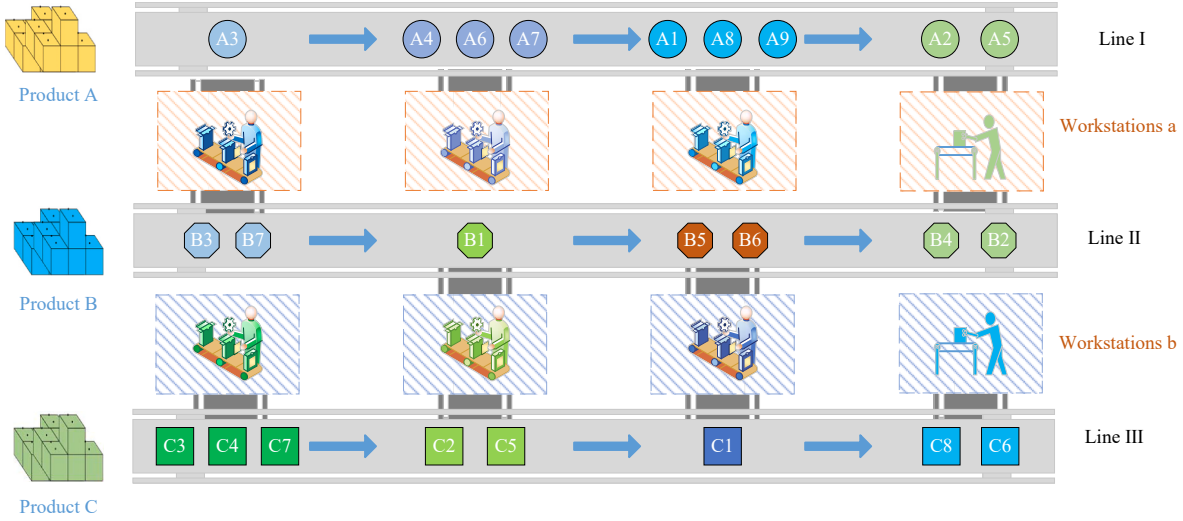

Fig. 2. Layout of multi-parallel disassembly line.

$$PF = \max \left(\begin{array}{l} \sum_{l=1}^{\|\boldsymbol{L}\|} \sum_{i=1}^{n} \left(\sum_{r\in\{\boldsymbol{R}|r+1\geq l\geq r\}} \sum_{k=1}^{m} \sum_{o=1}^{\|\boldsymbol{O}\|} x_{iko}^{lr} \cdot f_i^l \right) - \sum_{r=1}^{\|\boldsymbol{R}\|} \sum_{k=1}^{m} S_k^r \cdot CT \cdot cw - \sum_{l=1}^{\|\boldsymbol{L}\|} \sum_{i=1}^{n} \left(h_i^l \cdot t_i^l\right) \cdot ch \\ - \sum_{l=1}^{\|\boldsymbol{L}\|} \sum_{i=1}^{n} \left(\sum_{r\in\{\boldsymbol{R}|r+1\geq l\geq r\}} \sum_{k=1}^{m} \sum_{o=1}^{\|\boldsymbol{O}\|} x_{iko}^{lr} \cdot d_i^l \cdot t_i^l \right) \cdot cd \end{array} \right) \tag{4}$$

workers' idle time in each shared workstation. Eq. (3) minimises the energy consumption, including energy consumption for workstation working and auxiliary equipment such as ventilation and lighting, and extra energy consumption for separating hazardous and in-demand tasks. Finally, Eq. (4) maximises the total profit, i.e., maximises gross receipts and minimises disassembly costs. The disassembly costs include workstation working cost and extra costs for separating hazardous and demand tasks. Here, the energy consumption and cost for separating hazardous tasks are constant because the hazardous tasks must be removed. However, this portion of energy consumption and cost are still optimised as they are part of the objectives.

Eqs. (5) and (6) express the partial disassembly constraints. Hazardous tasks must be disassembled to prevent them causing pollution to the environment, and tasks without hazards may be disassembled.

$$\sum_{r\in\{\boldsymbol{R}|r+1\geq l\geq r\}} \sum_{k=1}^{m} x_{ik}^{lr} \leq 1, \forall i \in \boldsymbol{I}; \forall l \in \boldsymbol{L} \tag{5}$$

$$\sum_{r\in\{\boldsymbol{R}|r+1\geq l\geq r\}} \sum_{k=1}^{m} x_{ik}^{lr} = 1, \forall i, l \in \left\{\boldsymbol{I}, \boldsymbol{L} \middle| h_i^l \geq 1\right\} \tag{6}$$

Eqs. (7) and (8) express the order constraints of the disassembled tasks in each shared workstation.

$$\sum_{l\in\{\boldsymbol{L}|r+1\geq l\geq r\}} \sum_{i=1}^{n} x_{iko}^{lr} \leq 1, \forall r \in \boldsymbol{R}; \forall k \in \boldsymbol{M}; \forall o \in \boldsymbol{O} \tag{7}$$

$$x_{ik,o}^{lr} \leq x_{jk,o-1}^{ur}, \forall l \in \boldsymbol{L}; \forall r \in \{\boldsymbol{R}|r+1 \geq l \geq r\}; \forall u \in \{\boldsymbol{L}|r+1 \geq u \geq r\}; \\ \forall i, j \in \boldsymbol{I}; \forall r \in \boldsymbol{R}; \forall k \in \boldsymbol{M}; \forall o \in \{2, \ldots, m\} \tag{8}$$

Eq. (9) expresses the non-overlapping constraint for disassembled tasks. All tasks that need to be separated must be disassembled sequentially.

$$\alpha \cdot \left(2 - x_{ik,o-1}^{lr} - x_{jko}^{ur}\right) + w_j^u \geq w_i^l + t_i^l, \forall i, j \in \boldsymbol{I}; \forall l \in \boldsymbol{L}; \forall r \in \{\boldsymbol{R}|r+1 \geq l \geq r\}; \\ \forall u \in \{\boldsymbol{L}|r+1 \geq u \geq r\}; \forall k \in \boldsymbol{M}; \forall o \in \{2, \ldots, m\} \tag{9}$$

Eqs. (10)–(12) express the CT constraints. For standardized production lines, the total operation time of each shared workstation cannot exceed a CT, and both the beginning and ending operation time of disassembled tasks must meet CT constraints.

$$\sum_{l=1}^{\|\boldsymbol{L}\|} \sum_{i=1}^{n} \sum_{o=1}^{\|\boldsymbol{O}\|} \left(x_{iko}^{lr} \cdot t_i^l\right) \leq CT, \forall k \in \boldsymbol{M}, \forall r \in \boldsymbol{R} \tag{10}$$

$$CT \cdot \sum_{k=1}^{m} \sum_{r\in\{\boldsymbol{R}|r+1\geq l\geq r\}} \sum_{o=1}^{\|\boldsymbol{O}\|} \left(x_{iko}^{lr} \cdot (k-1)\right) \leq w_i^l + \alpha \cdot \left(1 - \sum_{k=1}^{m} \sum_{r\in\{\boldsymbol{R}|r+1\geq l\geq r\}} \sum_{o=1}^{\|\boldsymbol{O}\|} x_{iko}^{lr}\right), \forall i \in \boldsymbol{I}; \forall l \in \boldsymbol{L} \tag{11}$$

$$w_i^l + t_i^l \leq CT \cdot \sum_{k=1}^{m} \sum_{r\in\{\boldsymbol{R}|r+1\geq l\geq r\}} \sum_{o=1}^{\|\boldsymbol{O}\|} \left(x_{iko}^{lr} \cdot k\right) + \alpha \cdot \left(1 - \sum_{k=1}^{m} \sum_{r\in\{\boldsymbol{R}|r+1\geq l\geq r\}} \sum_{o=1}^{\|\boldsymbol{O}\|} x_{iko}^{lr}\right), \forall i \in \boldsymbol{I}; \forall l \in \boldsymbol{L} \tag{12}$$

Eqs. (13) and (14) express the precedence relationship constraints. For any waste product, the successor task j must be disassembled later than the predecessor task i, and the predecessor task i must be separated if the successor task j needs to be separated.

$$\alpha \cdot \left(1 - \sum_{k=1}^{m} \sum_{r\in\{\boldsymbol{R}|r+1\geq l\geq r\}} \sum_{o=1}^{\|\boldsymbol{O}\|} x_{jko}^{lr}\right) + w_j^l \geq \left(w_i^l + t_i^l\right), \forall i, j \in \left\{\boldsymbol{I} \middle| \boldsymbol{TP}_{ij}^l = 1\right\}; \forall l \\ \in \boldsymbol{L} \tag{13}$$

$$\sum_{k=1}^{m} \sum_{r\in\{\boldsymbol{R}|r+1\geq l\geq r\}} \sum_{o=1}^{\|\boldsymbol{O}\|} x_{iko}^{lr} \geq \sum_{k=1}^{m} \sum_{r\in\{\boldsymbol{R}|r+1\geq l\geq r\}} \sum_{o=1}^{\|\boldsymbol{O}\|} x_{jko}^{lr}, \forall i, j \in \left\{\boldsymbol{I} \middle| \boldsymbol{TP}_{ij}^l = 1\right\}; \forall l \in \boldsymbol{L} \tag{14}$$

Eq. (15) expresses the number constraint of shared workstations. The maximum number of workable shared workstations does not exceed the number of tasks, and the minimum number of workable shared workstations is not less than those of shared workstations when each workstation is fully loaded.

$$\left\lceil \left(\sum_{k=1}^{m} \sum_{l\in\{\boldsymbol{L}|r+1\geq l\geq r\}} \sum_{i=1}^{n} \times \sum_{o=1}^{\|\boldsymbol{O}\|} x_{iko}^{lr} \cdot t_i^l \right) \Big/ CT \right\rceil \leq \sum_{k=1}^{m} S_k^r \leq \sum_{k=1}^{m} \sum_{l\in\{\boldsymbol{L}|r+1\geq l\geq r\}} \sum_{i=1}^{n} \sum_{o=1}^{\|\boldsymbol{O}\|} x_{iko}^{lr}, \forall r \in \boldsymbol{R} \tag{15}$$

Eqs. (16) and (17) express the constraints of shared workstations being activated. First, the shared workstation is only activated when it has been assigned tasks. Then, each activated workstation is assigned at least one task.

$$S_k^r \leq \sum_{i=1}^{n} \sum_{l\in\{\boldsymbol{L}|r+1\geq l\geq r\}} \sum_{o=1}^{\|\boldsymbol{O}\|} x_{iko}^{lr}, \forall r \in \boldsymbol{R}; \forall k \in \boldsymbol{M} \tag{16}$$

$$n \cdot S_k^r \geq \sum_{i=1}^{n} \sum_{l\in\{\boldsymbol{L}|r+1\geq l\geq r\}} \sum_{o=1}^{\|\boldsymbol{O}\|} x_{iko}^{lr}, \forall r \in \boldsymbol{R}; \forall k \in \boldsymbol{M} \tag{17}$$

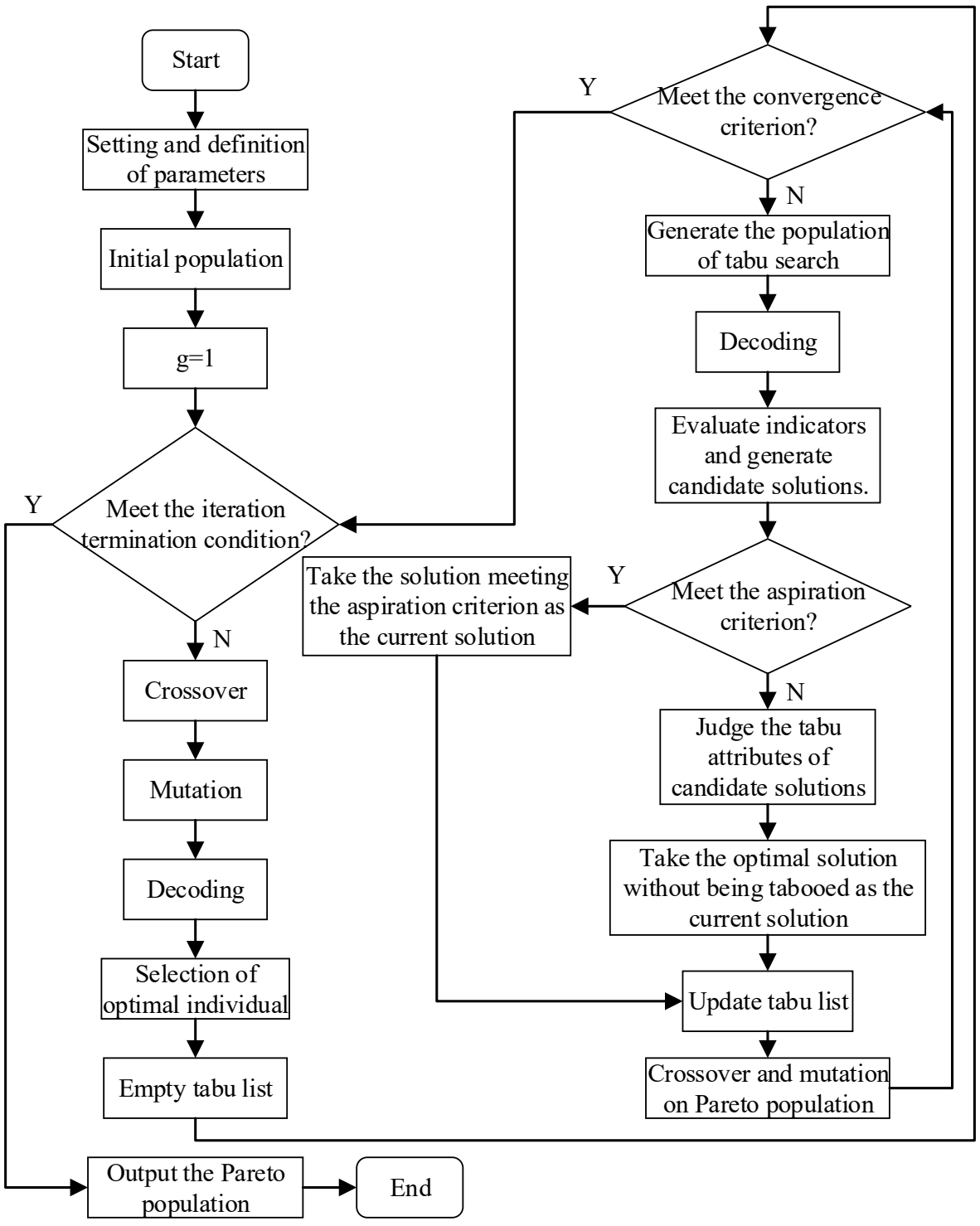

Fig. 4. Flow chart of GATS.

Eq. (18) express the constraint of shared workstations which are activated sequentially. A new shared workstation can only be activated when the preceding shared workstation has been activated.

$$S_k^r \le S_{k-1}^r, \forall r \in \boldsymbol{R}; \forall k \in \{2, \ldots, m\} \tag{18}$$

Eq. (19) expresses the binary variables of this model.

$$x_{iko}^{lr}, S_k^r \in \{0, 1\}, \forall i \in \boldsymbol{I}; \forall k \in \boldsymbol{M}; \forall o \in \boldsymbol{O}; \forall l \in \boldsymbol{L}; \forall r \in \boldsymbol{R} \tag{19}$$

4. Genetic and tabu search algorithm

The GA (Holland, 1992) was introduced by Prof. Holland and has been widely studied for its effectiveness in solving NP problems. Meanwhile, the tabu search algorithm (TS) (Glover, 1994) was introduced by Prof. Glover and has the advantage of prohibiting the repetition of local optima. The genetic and tabu search algorithm (GATS) combines the ability of the GA in a quick search for the optimum and the advantage of the TS, which can skip the local optimum. However, GATS which has superior performance never been applied to solve the DLBP.

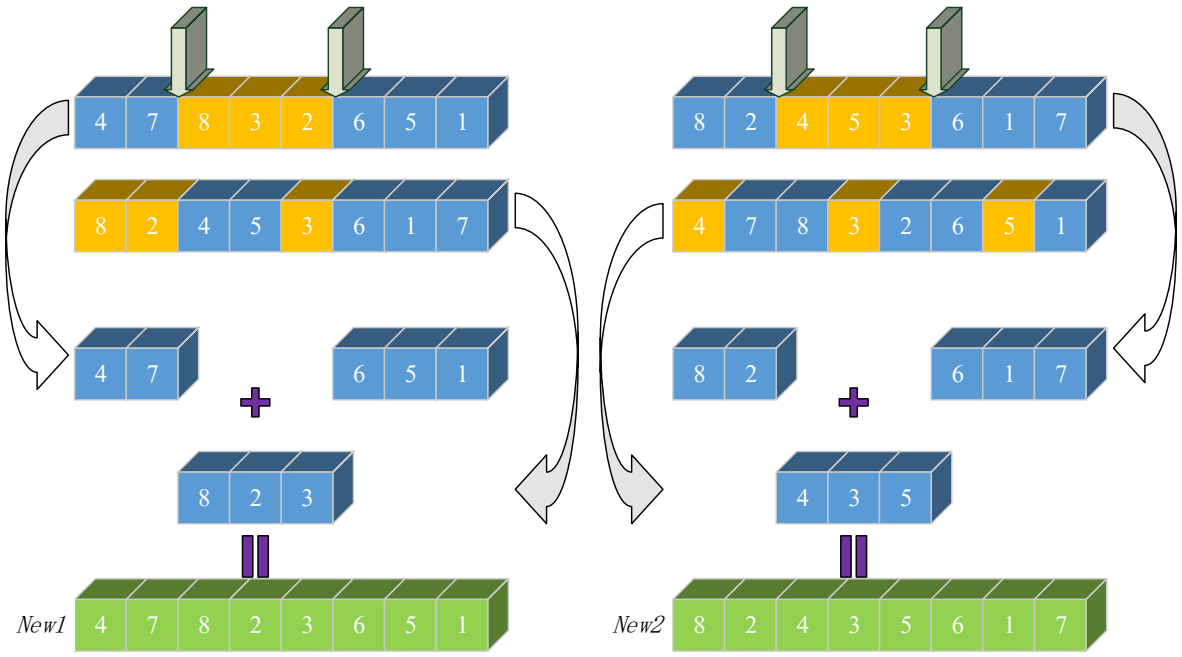

Fig. 5. Crossover operation.

In this study, GATS designed encoding and decoding mechanisms and an algorithmic framework applicable to MPPDLBP. The flow chart of the GATS is shown in Fig. 4.

4.1. Crossover

The crossover operation is shown in Fig. 5. Initially, individuals in the population are pairwise manipulated. Next, a random number generated within the range (0,1) is determined whether it satisfies the crossover criterion (random number less than the crossover probability). The crossover operation shown in Fig. 5 is executed when the crossover criterion is satisfied, then two new individuals are generated. In Fig. 5, two random points on the individual are selected, and tasks between two random points are rearranged following the order of the paired individual.

4.2. Mutation

The mutation operation adopts the single-point mutation, as shown in Fig. 6. The individual performs a mutation operation when the random number of corresponding task is smaller than the mutation probability. However, the predecessor and successor tasks of the selected task should be identified before the mutation operation is performed. Then, the selected task is randomly inserted into one of the positions between the predecessor and successor tasks.

4.3. Population generation for tabu search

The best individual in each iterative population after crossover and mutation is selected by the evaluation function. Then the population of the tabu search operation is generated by performing the mutation operation for the selected individual.

4.4. Evaluation function

The hyper-volume (*HV*) index (Bader and Zitzler, 2011) is employed as an evaluation function in the tabu search operation. The formula of the *HV* index is shown in Eq. (20). The value of the *HV* index represents the distance of the solution from the Pareto front. The greater the *HV* value, the better the comprehensive performance of the solution.

$$HV = volume\left(\bigcup_{i=1}^{n} V_i\right) \tag{20}$$

4.5. Encoding

Although MPPDLBP studies on the partial disassembly mode, the encoding of the complete disassembly mode is adopted. The precedence relationship matrix is merged using a diagonal approach. If the task indexes for waste products on three parallel lines are n_1, n_2, and n_3, the task indexes after merging are $1\sim n_1$, $n_1+1\sim n_1+n_2$, and $n_1+n_2+1\sim n_1+n_2+n_3$, respectively. The pseudocode of encoding is as follows:

Input: Precedence relationship matrix of three waste products and task scale n
(1) Three precedence relationship matrices are merged as ***TP***.
(2) **For** $i = 1$ to n
(3) A task in which the sum of column is 0 in the ***TP*** is randomly selected for the assignment.
(4) All row elements of ***TP*** corresponding to the selected task's serial number are replaced by 0.
(5) All column elements of ***TP*** corresponding to the selected task's serial number are replaced by 1.
(6) The selected task is saved to the disassembly sequence
(7) End **For** n
Output: A disassembly sequence

4.6. Decoding

Because the maximum profit and minimum energy consumption of a disassembly sequence need to be evaluated, the objective values for all disassembly levels need to be calculated and stored during decoding process. Each shared workstation is sequentially assigned a continuous segment of the disassembly sequence. Meanwhile, the continuous segment only can consist of tasks from two adjacent parallel lines. In addition, the tasks in the disassembly sequence are sequentially assigned backward while satisfying the *CT* constraints. If the assigned task that will be assigned does not belong to the two adjacent parallel lines or does not meet the *CT* constraints, the task assignment for the current shared workstation will be terminated. Then, a new shared workstation is activated, and this task will be assigned to the new activated

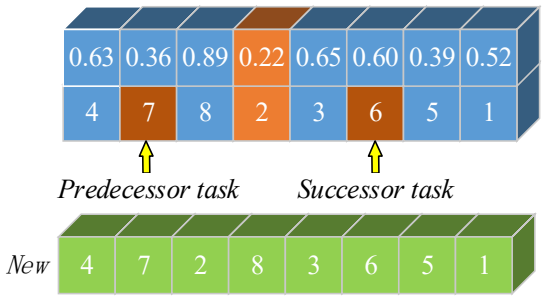

Fig. 6. Mutation operation.

Table 2
Disassembly information of three waste products.

P5				P6				P8			
t	H	D	f	t	H	D	f	t	H	D	f
16	0	1	3.53	7	0	0	1.94	9	0	0	1.73
20	0	1	3.78	6	0	0	0.85	5	1	1	2.34
8	0	1	2.84	5	0	1	3.61	7	0	1	4.57
4	1	1	0.68	5	0	1	2.03	8	0	0	1.33
10	0	1	2.12	5	1	0	1.11	6	0	0	3.07
				7	0	0	1.54	3	0	1	3.23
								4	0	0	1.57
								5	0	1	4.76

workstation. After all tasks have been assigned, the objective values of each disassembly level will be calculated and stored. Finally, the disassembly levels with best objective values for the disassembly sequence are selected, and the disassembled tasks are determined. Hence, four disassembly schemes can be obtained by decoding one disassembly sequence. The pseudocode of the decoding process is as follows:

Input: A disassembly sequence, precedence relationship matrix (*TP*), disassembly information matrix (*KB*), task scale (*n*), and *CT*
(1) Initialise all parameters.
(2) **For** all tasks
(3) Judge the current task belongs to which disassembly line.
(4) If the current task belongs to disassembly line I, then this task is assigned to a shared workstation in the first column; Otherwise, step (10) is performed.
(5) **For** the remainder tasks
(6) If the current task belongs to line III or does not meet the *CT* constraints, this loop is terminated, and a new shared workstation is activated. Then, the current task enters the main loop and is judged again.
(7) If the current task belongs to disassembly line I and meets the *CT* constraints, it is assigned to the current workstation.
(8) End **For**
(9) If the current task belongs to disassembly line III, its operation is similar to steps (5)–(8).
(10) If the current task belongs to disassembly line II, this task is assigned to a shared workstation in the second column; Otherwise, step (17) is performed.
(11) **For** the remainder tasks
(12) If the current task is still a task of line II, judge whether it meets the *CT* of the shared workstation in the second column.
(13) If the current task meets the *CT* constraints, the task assignment is saved; Otherwise, the saved tasks are assigned to the column with the maximum number of shared workstations.

(*continued on next column*)

(*continued*)

(14) If the current task belongs to line I and meets the *CT* constraints, the saved task assignment is assigned to the shared workstation in the first column.
(15) If the current task belongs to line III and meets the *CT* constraints, the saved task assignment is assigned to the shared workstation in the second column.
(16) End **For**
(17) The current task is assigned to a shared workstation in the second column.
(18) **For** the remainder tasks
(19) If the current task belongs to line I or does not meet the *CT* constraints, this loop is terminated, and a new shared workstation is activated. Then, the current task enters the main loop and is judged again.
(20) If the current task belongs to line III and meets the *CT* constraints, it is assigned to the currently workstation.
(21) End **For**
(22) End **For**
(23) Calculate the objective values corresponding to each disassembly level.
(24) Determine the best disassembly levels for each objective of the current disassembly sequence.

Output: Assignment information of disassembled tasks, activated information of shared workstations, best disassembly levels of current sequence, and objective values corresponding to the best disassembly levels

5. Model solution and algorithm verification

To verify the effectiveness of the GATS and the validity of the encoding and decoding mechanism, the GATS is compared with the MINLP model. However, the MPPDLBP has not been investigated in any study. Thus, the GATS is compared with several existing algorithms for solving the straight layout. In addition, the solver software of the MINLP model is GUROBI 9.1.1 optimiser, and the solver software of the GATS is MATLAB 2014b. The running environment is Windows 7, Intel(R) Xeon (R) CPU E5–1620 v3 @ 3.50 GHz, 32 GB RAM.

5.1. MINLP model solution

The MINLP model and the GATS are applied to solve a hybrid disassembly instance consisting of P5 (Xiao et al., 2019), P6 (Zhu et al., 2020b), and P8 (Zhu et al., 2020b). The disassembly information of above three waste products is shown in Table 2, and the precedence relationship diagrams are shown in Fig. 7. Additionally, P5, P8, and P6 are separated on parallel lines I, II, and III, respectively. The cycle time is set as $CT = 40$ s.

The energy consumption and cost parameters are set as follows: $ew = 0.12$ kJ/s, $el = 0.05$ kJ/s, $eh = 0.03$ kJ/s, $ed = 0.01$ kJ/s, $cw = 0.13$ Yuan/s, $ch = 0.01$ Yuan/s, and $cd = 0.01$ Yuan/s. The computational results of the MINLP model and GATS are shown in Table 3. The best values of each objective in Table 3 is highlighted in bold.

As indicated in Table 3, both the MINLP model and GATS obtained the best values of each objective. Furthermore, the GATS obtained eight non-dominant solutions containing the optimal values of single-objective. The Gantt charts of optimal values for each objective are plotted as shown in Fig. 8. In Fig. 8, WA and WB indicate the shared workstations in the first and second columns, respectively. In addition, the light green rectangles represent the tasks of P5, the dark green rectangles represent the tasks of P6, and the purple rectangles represent the tasks of P8. Fig. 8 demonstrates that the tasks are reasonably

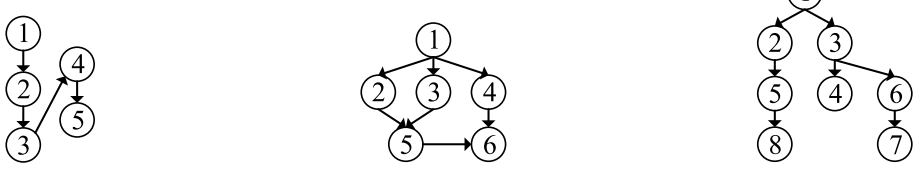

(a) P5 (b) P6 (c) P8

Fig. 7. Precedence relationship diagrams of three waste products.

Table 3
Computational results of the MINLP model and GATS.

Instance	MINLP				GATS			
	WT	TB	EC	PF	WT	TB	EC	PF
P5+P6+P8	**3**	–	–	–	**3**	37	21.50	19.76
					3	**1**	21.55	20.21
	–	**1**	–	–	**3**	77	**21.40**	9.16
					3	11	21.60	**25.12**
	–	–	**21.40**	–	**3**	2	21.55	24.47
					3	14	21.47	13.66
	–	–	–	**25.12**	**3**	22	21.45	11.14
					3	25	21.50	19.76

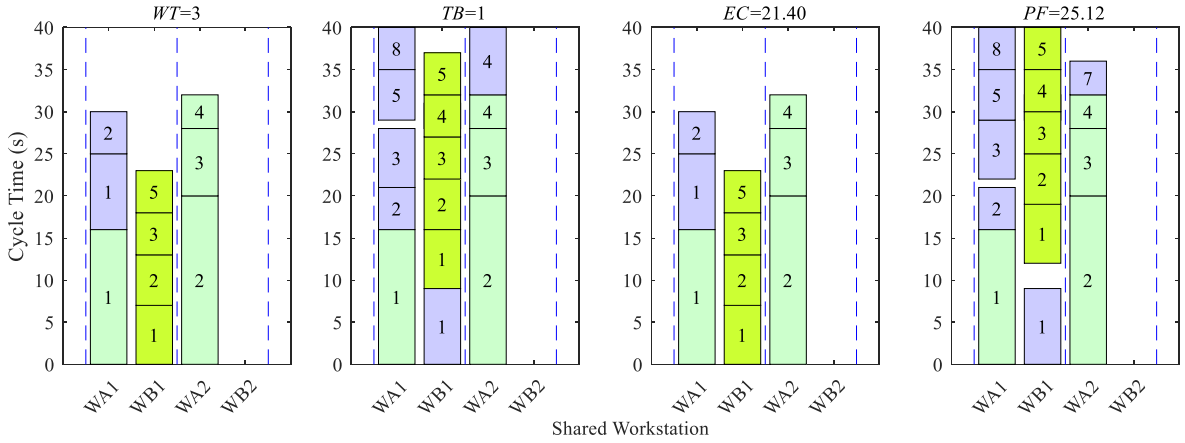

Fig. 8. Gantt charts of optimal values for each objective.

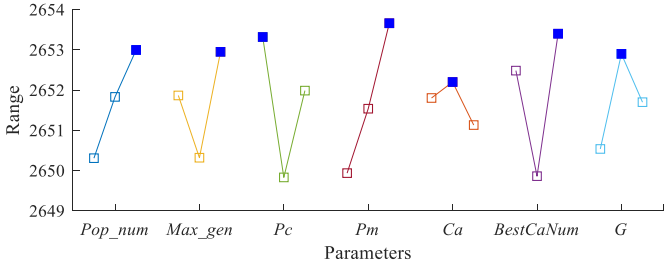

Fig. 9. Level trends of parameters for GATS.

assigned, and no overlap or disorder. Therefore, the correctness of encoding and decoding mechanism is verified.

5.2. Algorithm comparison

To verify the performance of the applied algorithm, the GATS is compared with several existing algorithms. Because of no literature on the MPPDLBP, the GATS is compared with the solution methods of solving the straight DLBP, which has been studied widely. Therefore, a P52 test case (Ding et al., 2009) is optimised. In particular, four existing solution methods, namely, the multi-objective ant colony algorithm (MACO) (Ding et al., 2009), ant colony genetic algorithm (ACGA) (Zhang et al., 2018), genetic simulated annealing algorithm (GASA) (Wang et al., 2017), and local neighbourhood genetic algorithm (LNGA) (Zhang et al., 2019), are compared. Meanwhile, three optimisation objectives are the same as those in the original literature, which are still F_{Idle}, F_{Smooth}, and F_{Cost}. In addition, the computational results of four comparison algorithms are derived from the original literature.

Because GATS has seven parameters, the orthogonal table L_{18} (3^7) is chosen for the parameter experiments. First, the levels of the seven parameters are set as follows: *Pop_num* ∈ {100, 80, 120} (the number of population), *Max_gen* ∈ {5, 6, 7} (the maximum number of iterations), *Pc* ∈ {0.9, 0.7, 0.8} (crossover probability), *Pm* ∈ {0.2, 0.3, 0.4} (mutation probability), *Ca* ∈ {100, 120, 80} (the number of neighbourhood solutions), *BestCaNum* ∈ {30, 60, 120} (the number of candidate solutions), *G* ∈ {50, 150, 100} (the number of tabu searches). After the orthogonal designs, the level trends of seven parameters are displayed in Fig. 9. Then, the algorithm parameters of the GATS are set as follows: *Pop_number* = 120, *Max_gen* = 7, *Pc* = 0.9, *Pm* = 0.4, *Ca* = 120, *BestCaNum* = 120, and *G* = 150. Finally, the computational results of GATS are listed in Table 4, and the best values of each objective in Table 4 are highlighted in bold.

The box plots of three objectives and the *HV* indexes of five algorithms are shown in Fig. 10. For the objective F_{Idle}, the best values obtained by the five algorithms all are 0.0579. For objectives F_{Smooth} and F_{Cost}, the best values obtained by the GATS are 1.00 and 125.868, respectively, both outperforming the best values of (0.9747, 0.9900, 0.9974, and 0.9999) and (150.546, 130.332, 133.824, and 127.146) obtained by other four compared algorithms. In addition, the GATS

Table 4
Computational results of GATS.

Objective	1	2	3	4	5	6	7	8	9	10
F_{Idle}	**0.0579**	**0.0579**	**0.0579**	**0.0579**	**0.0579**	**0.0579**	**0.0579**	**0.0579**	**0.0579**	**0.0579**
F_{Smooth}	0.8607	0.9192	0.9998	0.9260	**1.0000**	0.9397	0.8804	0.9973	0.9980	0.9986
F_{Cost}	**125.868**	128.550	140.304	128.628	141.594	129.726	127.776	129.750	129.096	131.196

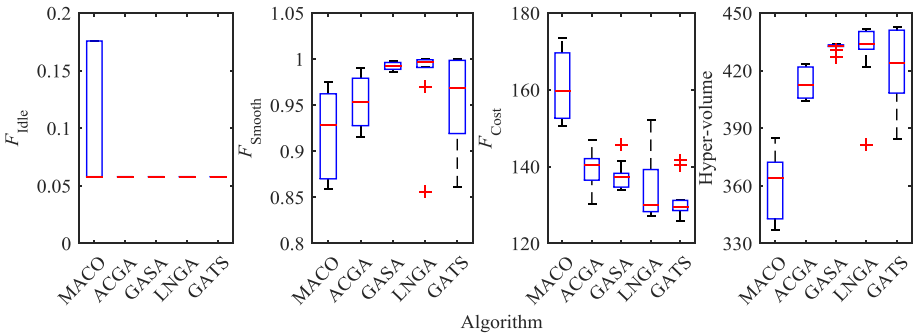

Fig. 10. Box plots of computational results of five algorithms.

Table 5
Information of three waste products.

ID	P27					P25					P22				
	t	*H*	*D*	*f*	Predecessor tasks	*t*	*H*	*D*	*f*	Predecessor tasks	*t*	*H*	*D*	*f*	Predecessor tasks
1	50	0	0	1.37	–	47	0	0	1.00	–	15	0	0	1.33	–
2	9	0	0	1.70	1	24	1	0	2.21	–	9	0	0	1.48	1
3	3	0	0	0.86	2	10	0	0	2.23	2	3	0	0	2.91	2
4	7	0	1	3.82	2	20	0	0	1.57	3	7	0	1	3.94	2
5	24	0	0	2.92	2	16	0	0	2.88	4	12	0	0	3.40	2
6	2	1	0	2.43	7	20	1	0	1.53	5	2	1	0	2.91	5,7
7	10	0	0	1.27	2	20	1	0	0.93	6	10	0	0	2.69	2
8	18	0	1	3.16	15	75	1	1	4.95	1	4	0	0	1.41	5
9	4	0	1	3.42	15	30	0	0	2.67	8	4	0	1	4.05	8
10	4	0	0	2.19	5	7	0	0	2.84	8	4	0	0	3.61	8
11	4	0	1	3.48	10	15	0	1	4.85	10	4	1	1	1.17	8
12	4	0	0	2.55	10	10	0	0	3.60	9,11	4	1	0	0.95	5
13	4	1	1	4.03	10	28	1	0	2.23	12	4	0	0	2.37	12
14	4	1	1	3.79	10	20	0	0	1.68	2	4	0	1	4.69	11
15	4	1	0	2.18	5	25	0	0	2.87	14	1	0	0	2.10	–
16	4	0	0	1.66	15	18	0	0	3.28	2	7	1	0	2.13	8,13
17	4	0	1	3.38	13	18	0	0	2.19	16	3	1	0	2.84	16
18	4	0	0	2.30	10	7	0	0	2.94	2	3	1	0	1.17	17
19	17	0	0	0.91	2	15	0	1	4.51	18	1	0	0	1.56	17
20	16	0	0	2.78	19	10	0	0	2.31	2	2	0	0	2.30	17
21	7	1	0	2.06	16,19	5	0	0	2.73	2	2	0	1	4.49	17
22	3	1	0	1.60	21	25	0	1	4.33	15,17,19,20,21	2	0	0	1.92	18
23	3	1	0	1.61	22	40	0	0	2.82	13					
24	4	0	0	2.60	22	60	1	1	4.12	23					
25	2	0	0	2.10	22	28	0	0	1.40	22					
26	2	0	1	4.39	22										
27	2	0	0	2.91	23										

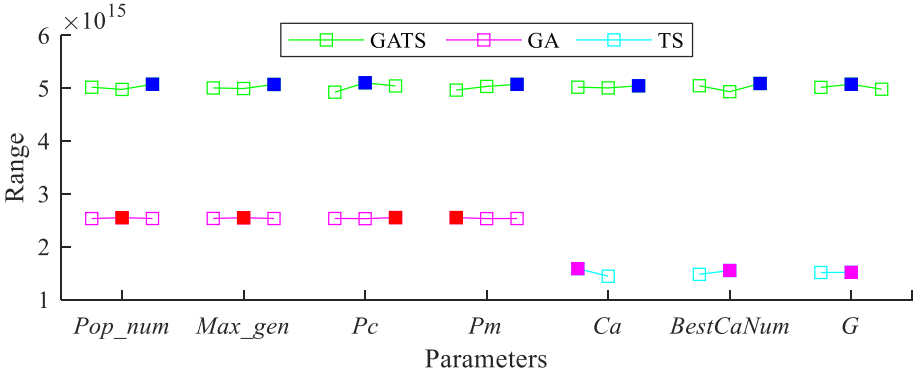

Fig. 11. Level trends of parameters of GATS, GA, and TS.

obtained ten groups of non-dominated solutions. But MACO and ACGA only obtained seven and eight groups of non-dominated solutions, respectively. For the *HV* index, the GATS obtained the maximum *HV* value, and the upper quartile line of the GATS outperforms other four compared algorithms. Moreover, the box plot of *HV* values for the GATS shows no outliers. Thus, the GATS exhibited superior performance in solving the DLBP.

6. Instance application and analysis

The GATS is applied to optimise a MPPDLBP instance consisting of two types of waste televisions (P22 and P27) and one type of waste

Table 6
Parameters of three algorithms.

Algorithm	*pop_number*	*Max_gen*	*Pc*	*Pm*	*Ca*	*BestCaNum*	*G*
GATS	200	50	0.7	0.4	800	800	50
GA	240	350	0.7	0.4	–	–	–
TS	–	–	–	–	1200	1200	1000

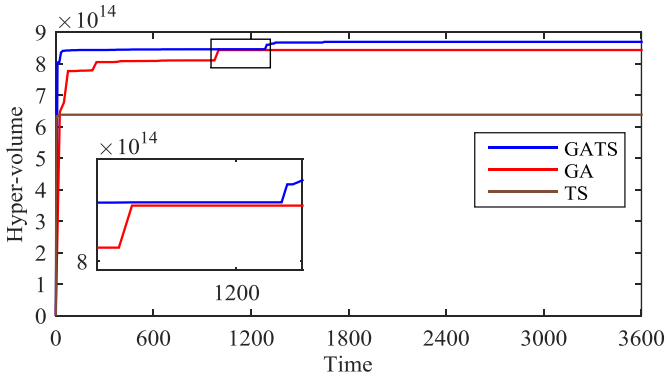

Fig. 12. *HV* iteration diagram of the three algorithms.

refrigerator (P25). The information of three waste products is presented in Table 5. For three waste products, P27 is separated on the middle parallel line, P22 and P25 are separated on the two side parallel lines, respectively. The *CT* is set as 130s, and the parameters of energy consumption and cost are the same as in Section 5.1.

In addition, the GA and TS are employed to optimise this instance to further verify the performance of the GATS. The parameters of three algorithms are set by orthogonal designs. The parameters of GATS are still experimented according to orthogonal table L_{18} (3^7). The levels of seven parameters for GATS are set as follows: *Pop_num* ∈ {100, 80, 120}, *Max_gen* ∈ {5, 6, 7}, *Pc* ∈ {0.9, 0.7, 0.8}, *Pm* ∈ {0.2, 0.3, 0.4}, *Ca* ∈ {100, 120, 80}, *BestCaNum* ∈ {30, 60, 120}, and *G* ∈ {50, 150, 100}. The parameters of GA are experimented according to the orthogonal table L_9 (3^4). The levels of four parameters for GA are set as follows: *Pop_num* ∈ {220, 240, 200}, *Max_gen* ∈ {450, 350, 400}, *Pc* ∈ {0.8, 0.9, 0.7}, and *Pm* ∈ {0.4, 0.3, 0.2}. The parameters of TS are experimented according to the orthogonal table L_4 (2^3). The levels of three parameters for TS are set as follows: *Ca* ∈ {1200, 1000}, *BestCaNum* ∈ {600, 1200}, and *G* ∈ {1200, 1000}. The level trends of parameters for GATS, GA, and TS are displayed in Fig. 11. The corresponding levels for each parameter are the same as those mentioned above. The parameter level with the best experimental values is the best parameter combination. The best parameters for GATS, GA, and TS are highlighted in blue, red, and pink, respectively. Based on the orthogonal designs, the parameters of three algorithms are shown in Table 6.

Fig. 12 illustrates the iterative diagram of the three algorithms within 3600s. As displayed in Fig. 12, the GATS obtained the maximum *HV* index in the shortest time. Although the GATS eventually converged later than the GA and TS, the *HV* value obtained by the GATS is significantly better than those obtained by the GA and TS. Thus, the GATS is superior in solving MPPDLBP.

The computational results of the GATS are shown in Table 7. For four optimisation objectives, the values of the number of workstations are all 7, the values of the workstation load balancing index, energy consumption, and profit range from 5 to 1035, 165 to 165.59, and 28.14 to 66.51, respectively. Therefore, decision-makers can select a reasonable disassembly scheme based on the requirements of recycling enterprises. Moreover, Fig. 13 shows the trend diagrams of each objective at the disassembly level of scheme 2. The mandatory disassembled tasks for scheme 2 are the first 60 tasks. In Fig. 13, the number of shared workstations, energy consumption, cost, and gross receipt indexes rise with the increasing number of tasks. The profit peaks several times during decoding process, but the maximum peak occurs at the 74th task. The workstation load balancing index is related to the number of shared workstations and tasks. As a result, the workstation load balancing index increases dramatically when a new shared workstation is activated. However, the workstation load balancing index tends to decrease as tasks are continuously assigned to the shared workstations. Thus, scheme 2 is one of the most profitable schemes for recycling enterprises aiming to achieve both maximise profits and sustainable development.

7. Conclusions and future research

This study designed the reasonable encoding and decoding

Table 7
Computational results of GATS.

ID	*WT*	*TB*	*EC*	*PF*	Scheme
1	**7**	1035	**165**	30.53	WA: [1,2,23,24,7,27,5]→[3,6,30,8,12,13,31,11,16,17,18,22,38,20,35,19,10,43,40,44,15,45,34,46,47,25,49,36] WB: [50,51,67,41,63,37,32]→[57,58,70,59]→[65,52,29,53,60,66,61,68]→[64,69,62,54,72]→[55,56,73,28,42]
2	**7**	31	165.59	**66.51**	WA: [1,23,2,15,24,7,27,5]→[6,30,8,12,13,31,11,16,17,18,3,22,20,38,35,43,10,44,45,47,46,40,19,49,25,14,21,9,4,48,39,34] WA:0 [1,23,2,15,24,7,27,5]→[6,30,8,12,13,31,11,16,17,18,3,22,20,38,35,43,10,44,45,47,46,40,19,49,25,14,21,9,4,48,39,34] WB: [50,51,67,41,63,37,32]→[57,58,70,65]→[59,52,53,60,29,61,68,64,36,69,28]→[62,66,71,54,72]→[26,55,56,73,42,33]
3	**7**	371	165.11	28.14	WA: [1,23,2,24,7,27,5]→[3,6,30,8,12,13,31,11,16,17,18,38,20,15,36,43,10,39,44,45,46,40,19] WB: [50,51,67,41,63,37,32]→[57,58,35,70,59]→[65,52,53,60,29,61,68,64]→[69,28,62,66,25,26,54,72]→[55,56,73,42]
4	**7**	**5**	165.41	48.10	WA: [1,2,23,15,24,7,27,5]→[3,6,4,30,8,12,13,31,11,42,16,17,18,22,10,38,35,19,20,43,40,44,45,34,47,46,25,49,21] WB: [50,51,67,41,63,37,32]→[26,57,58,65]→[59,52,29,53,60,66,61,68,64]→[69,28,70,36,62,71,54,72]→[55,56,73,74]
5	**7**	**5**	165.57	60.76	WA: [23,1,2,15,24,7,27,5]→[3,6,4,30,8,12,13,31,11,16,17,18,22,38,35,14,43,10,40,20,39,44,45,34,25,46,19,47,33,49,9,21] WB: [50,51,67,41,63,37,32]→[26,57,58,65]→[59,52,29,53,60,66,61,68,64]→[69,28,70,36,62,71,54,72]→[55,56,73,74]
6	**7**	24	165.59	62.83	WA: [1,2,15,23,24,7,27,5]→[6,30,8,12,13,11,31,16,17,4,18,22,38,19,35,43,34,44,45,10,20,46,21,47,3,9,14,39,33,48,49,36] WB: [50,51,70,67,41,63,37,32]→[57,58,65,59]→[52,53,60,29,61,68,64,69,25,28,26]→[62,66,71,54,72]→[55,74,56,73]
7	**7**	891	165.04	39.37	WA: [1,2,23,24,7,27,5]→[3,6,30,8,12,13,31,11,16,17,18,22,10,38,35,21,20,19,43,40,44,15,45,34,47,46,25,48,49,36] WB: [50,51,67,41,63,37,32]→[57,58,70,59]→[65,52,29,53,60,66,61,68]→[64,69,62,54,72]→[55,56,73,28,42]
8	**7**	499	165.04	33.87	WA: [1,2,23,24,7,27,5]→[3,6,30,8,12,13,31,11,16,17,18,19,38,39,20,43,40,44,15,45,10,47,46,25,49,22,36] WB: [50,51,67,41,63,37,32]→[57,35,58,70,59]→[65,52,29,53,60,66,61,68]→[64,28,69,62,54,72]→[55,56,73,34,42]
9	**7**	959	165.02	34.90	WA: [1,2,23,24,7,27,5]→[3,6,30,8,12,13,31,11,16,17,18,22,10,38,35,20,19,43,40,44,15,48,45,34,47,46,25,49,36] WB: [50,51,67,41,63,37,32]→[57,58,70,59]→[65,52,29,53,60,66,61,68]→[64,69,62,54,72]→[55,56,73,28,42]
10	**7**	74	165.25	36.01	WA: [23,1,2,24,7,27,5]→[6,30,8,12,13,31,11,16,17,18,22,38,3,25,19,35,43,34,44,45,10,20,46,49,47,15,40,42,36] WB: [50,51,67,41,63,37,32]→[57,58,65,70]→[59,52,53,60,29,61,68,64,69,28]→[62,66,71,54,72]→[55,56,73,74]

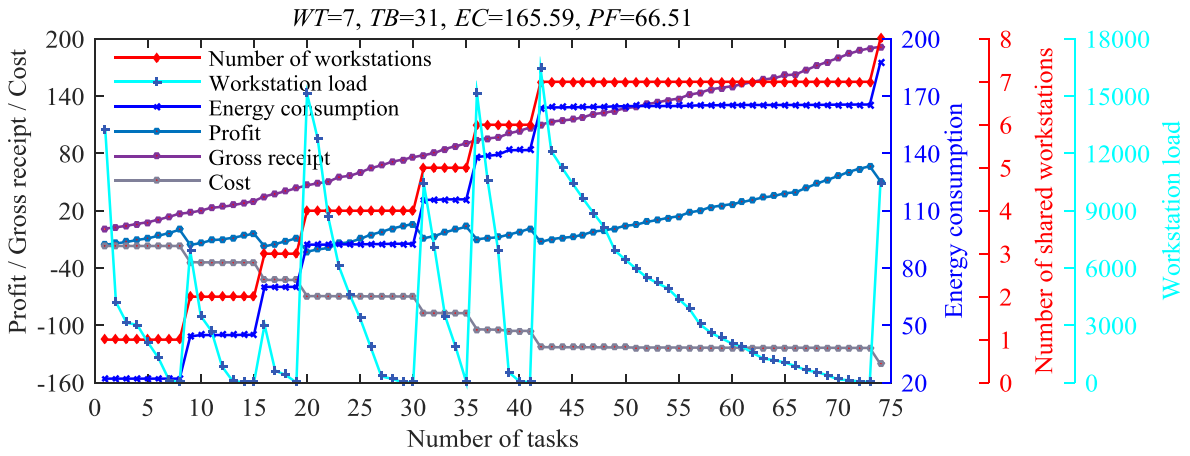

Fig. 13. Trend diagrams of each objective varies with disassembly levels.

mechanisms for the proposed MPPDLBP and verified its validity using the established MINLP model. Additionally, the proposed GATS hybrid algorithm was compared with the original GA and TS. The GATS proved superior to the GA and TS in optimisation capability within 3600s. The superiority of the GATS was validated by comparing it with several existing algorithms. Finally, ten disassembly schemes were provided for a hybrid waste products instance, and analyses of disassembly levels were shown for each objective. The analysis revealed that the partial disassembly mode could better achieve the maximum profit and minimum energy consumption for enterprises.

In addition, the model and algorithm proposed in this paper have meaningful management implications for the recycling industry and enterprises regarding decision-making, energy saving, and economics:

1. The proposed model and solution methods can help decision makers make decisions faster in assigning disassembly tasks and selecting disassembly schemes.
2. Various optimisation objectives benefit decision-makers who manage recycling enterprises' development directions better.
3. The research on the levels and economy of disassembly positively impacts the long-term development of recycling enterprises.

Numerous interesting research directions are available for the MPPDLBP in the future. For example, considering 'AND/OR' relationships (Paksoy et al., 2013) will make disassembly more complex but exciting. Furthermore, the decoding method designed in this study can be applied to solve MPPDLBP with more parallel lines. In addition, investigating the partial disassembly mode of other termination criteria is also meaningful.

Declaration of competing interest

None.

Data availability

Data will be made available on request.

Acknowledgements

This research was partially supported by the National Natural Science Foundation of China [Nos. 51205328, 51675450]; the Youth Foundation for Humanities, Social Sciences of Ministry of Education of China [No. 18YJC630255]; and the Sichuan Science and Technology Program [Nos. 2022YFG0245, 2022YFG0241]. In addition, we sincerely thank reviewers for their constructive comments on our paper.

References

Bader, J., Zitzler, E., 2011. HypE: an algorithm for fast hypervolume-based many-objective optimization. Evol. Comput. 19 (1), 45–76. https://doi.org/10.1162/EVCO_a_00009.

Battaïa, O., Dolgui, A., 2013. A taxonomy of line balancing problems and their solutionapproaches. Int. J. Prod. Econ. 142 (2), 259–277. https://doi.org/10.1016/j.ijpe.2012.10.020.

Battaïa, O., Dolgui, A., 2022. Hybridizations in line balancing problems: a comprehensive review on new trends and formulations. Int. J. Prod. Econ. 1–19. https://doi.org/10.1016/j.ijpe.2022.108673.

Bentaha, M.L., Battaïa, O., Dolgui, A., 2014. A sample average approximation method for disassembly line balancing problem under uncertainty. Comput. Oper. Res. 51, 111–122. https://doi.org/10.1016/j.cor.2014.05.006.

Bentaha, M.L., Battaïa, O., Dolgui, A., 2015. An exact solution approach for disassembly line balancing problem under uncertainty of the task processing times. Int. J. Prod. Res. 53 (6), 1807–1818. https://doi.org/10.1080/00207543.2014.961212.

Bentaha, M.L., Dolgui, A., Battaia, O., Riggs, R.J., Hu, J., 2018. Profit-oriented partial disassembly line design: dealing with hazardous parts and task processing times uncertainty. Int. J. Prod. Res. 56 (24), 7220–7242. https://doi.org/10.1080/00207543.2017.1418987.

Bentaha, M.L., Voisin, A., Marangé, P., 2020. A decision tool for disassembly process planning under end-of-life product quality. Int. J. Prod. Econ. 219, 386–401. https://doi.org/10.1016/j.ijpe.2019.07.015.

Ding, L.P., Tan, J.R., Feng, Y.X., Gao, Y.C., 2009. Multiobjective optimization for disassembly line balancing based on Pareto ant colony algorithm. Comput. Integr. Manuf. Syst. 15 (7), 1406–1413. https://doi.org/10.13196/j.cims.2009.07.160.dinglp.005.

Diri Kenger, Z., Koç, Ç., Özceylan, E., 2021. Integrated disassembly line balancing and routing problem with mobile additive manufacturing. Int. J. Prod. Econ. 235, 1–9. https://doi.org/10.1016/j.ijpe.2021.108088.

Edis, E.B., Ilgin, M.A., Edis, R.S., 2019. Disassembly line balancing with sequencing decisions: a mixed integer linear programming model and extensions. J. Clean. Prod. 238, 1–12. https://doi.org/10.1016/j.jclepro.2019.117826.

Edis, E.B., Sancar Edis, R., Ilgin, M.A., 2022. Mixed integer programming approaches to partial disassembly line balancing and sequencing problem. Comput. Oper. Res. 138, 1–14. https://doi.org/10.1016/j.cor.2021.105559.

Glover, F., 1994. Tabu search for nonlinear and parametric optimization (with links to genetic algorithms). Discrete Appl. Math. 49 (1–3), 231–255. https://doi.org/10.1016/0166-218X(94)90211-9.

Go, T.F., Wahab, D.A., Rahman, M.N.A., Ramli, R., Hussain, A., 2012. Genetically optimised disassembly sequence for automotive component reuse. Expert Syst. Appl. 39 (5), 5409–5417. https://doi.org/10.1016/j.eswa.2011.11.044.

Godichaud, M., Amodeo, L., 2018. Economic order quantity for multistage disassembly systems. Int. J. Prod. Econ. 199, 16–25. https://doi.org/10.1016/j.ijpe.2018.02.008.

Gupta, S.M., Gungor, A., 2001. Product recovery using a disassembly line: challenges and solution. In: Proceedings of the 2001 Ieee International Symposium on Electronics and the Environment, Conference Record, pp. 36–40. https://doi.org/10.1109/isee.2001.924499.

Hasegawa, S., Kinoshita, Y., Yamada, T., Bracke, S., 2019. Life cycle option selection of disassembly parts for material-based CO 2 saving rate and recovery cost: analysis of different market value and labor cost for reused parts in German and Japanese cases. Int. J. Prod. Econ. 213, 229–242. https://doi.org/10.1016/j.ijpe.2019.02.019.

He, J., Chu, F., Dolgui, A., Zheng, F., Liu, M., 2022. Integrated stochastic disassembly line balancing and planning problem with machine specificity. Int. J. Prod. Res. 60 (5), 1688–1708. https://doi.org/10.1080/00207543.2020.1868600.

Holland, J.H., 1992. Genetic algorithms. Sci. Am. 267 (1), 66–72. https://doi.org/10.1038/scientificamerican0792-66.

Kalayci, C.B., Gupta, S.M., 2013. A particle swarm optimization algorithm with neighborhood-based mutation for sequence-dependent disassembly line balancing

problem. Int. J. Adv. Manuf. Technol. 69 (1–4), 197–209. https://doi.org/10.1007/s00170-013-4990-1.
Kucukkoc, I., 2020. Balancing of two-sided disassembly lines: problem definition, MILP model and genetic algorithm approach. Comput. Oper. Res. 124, 1–17. https://doi.org/10.1016/j.cor.2020.105064.
Kucukkoc, I., Li, Z., Li, Y., 2020. Type-E disassembly line balancing problem with multi-manned workstations. Optim. Eng. 21 (2), 611–630. https://doi.org/10.1007/s11081-019-09465-y.
Li, Z., Janardhanan, M.N., 2021. Modelling and solving profit-oriented U-shaped partial disassembly line balancing problem. Expert Syst. Appl. 183, 1–13. https://doi.org/10.1016/j.eswa.2021.115431.
Liang, W., Zhang, Z., Zeng, Y., Yin, T., Wu, T., 2023a. Modeling and optimization of parallel disassembly line balancing problem with parallel workstations. IEEE Trans. Ind. Inf. 1–8. https://doi.org/10.1109/TII.2023.3241583.
Liang, W., Zhang, Z., Zhang, Y., Xu, P., Yin, T., 2023b. Improved social spider algorithm for partial disassembly line balancing problem considering the energy consumption involved in tool switching. Int. J. Prod. Res. 61 (7), 2250–2266. https://doi.org/10.1080/00207543.2022.2069059.
McGovern, S.M., Gupta, S.M., 2006. Ant colony optimization for disassembly sequencing with multiple objectives. Int. J. Adv. Manuf. Technol. 30, 481–496. https://doi.org/10.1007/s00170-005-0037-6.
Nahas, N., Nourelfath, M., Gendreau, M., 2014. Selecting machines and buffers in unreliable assembly/disassembly manufacturing networks. Int. J. Prod. Econ. 154, 113–126. https://doi.org/10.1016/j.ijpe.2014.04.011.
Paksoy, T., Gungor, A., Ozceylan, E., Hancilar, A., 2013. Mixed model disassembly line balancing problem with fuzzy goals. Int. J. Prod. Res. 51 (20), 6082–6096. https://doi.org/10.1080/00207543.2013.795251.
Pour-Massahian-Tafti, M., Godichaud, M., Amodeo, L., 2021. New models and efficient methods for single-product disassembly lot-sizing problem with surplus inventory decisions. Int. J. Prod. Res. 59 (22), 6898–6918. https://doi.org/10.1080/00207543.2020.1829148.
Ren, Y., Yu, D., Zhang, C., Tian, G., Meng, L., Zhou, X., 2017. An improved gravitational search algorithm for profit-oriented partial disassembly line balancing problem. Int. J. Prod. Res. 55 (24), 7302–7316. https://doi.org/10.1080/00207543.2017.1341066.
Ren, Y., Zhang, C., Zhao, F., Triebe, M.J., Meng, L., 2020. An MCDM-based multiobjective general variable neighborhood search approach for disassembly line balancing problem. IEEE Transactions on Systems, Man, and Cybernetics: Systems 50 (10), 3770–3783. https://doi.org/10.1109/TSMC.2018.2862827.
Smith, S., Hsu, L.Y., Smith, G.C., 2016. Partial disassembly sequence planning based on cost-benefit analysis. J. Clean. Prod. 139, 729–739. https://doi.org/10.1016/j.jclepro.2016.08.095.
Wang, K., Gao, L., Li, X., 2020. A multi-objective algorithm for U-shaped disassembly line balancing with partial destructive mode. Neural Comput. Appl. 32, 12715–12736. https://doi.org/10.1007/s00521-020-04721-0.
Wang, K., Li, X., Gao, L., Li, P., Sutherland, J.W., 2022. A discrete artificial bee colony algorithm for multiobjective disassembly line balancing of end-of-life products. IEEE Trans. Cybern. 52 (8), 7415–7426. https://doi.org/10.1109/TCYB.2020.3042896.
Wang, K., Zhang, Z., Zhu, L., Zou, B., 2017. Pareto genetic simulated annealing algorithm for multi objective disassembly line balancing problem. Comput. Integr. Manuf. Syst. 23 (6), 1277–1285. https://doi.org/10.13196/j.cims.2017.06.013.
Xia, X., Liu, W., Zhang, Z., Wang, L., 2020. Partial disassembly line balancing problem analysis based on sequence-dependent stochastic mixed-flow. J. Comput. Inf. Sci. Eng. 20 (6), 1–12. https://doi.org/10.1115/1.4046993.
Xiao, Q., Guo, X., Gu, X., 2019. The stochastic mixed-model U-shaped disassembly line balancing and sequencing optimization problem with multiple constraints. Ind. Eng. Manag. 24 (5), 87–96. https://doi.org/10.19495/j.cnki.1007-5429.2019.05.012.
Yin, T., Zhang, Z., Jiang, J., 2021. A Pareto-discrete hummingbird algorithm for partial sequence-dependent disassembly line balancing problem considering tool requirements. J. Manuf. Syst. 60, 406–428. https://doi.org/10.1016/j.jmsy.2021.07.005.
Yin, T., Zhang, Z., Zhang, Y., Wu, T., Liang, W., 2022. Mixed-integer programming model and hybrid driving algorithm for multi-product partial disassembly line balancing problem with multi-robot workstations. Robot. Comput. Integrated Manuf. 73, 1–18. https://doi.org/10.1016/j.rcim.2021.102251.
Zhang, Y., Zhang, Z., Guan, C., Xu, P., 2022. Improved whale optimisation algorithm for two-sided disassembly line balancing problems considering part characteristic indexes. Int. J. Prod. Res. 60 (8), 2553–2571. https://doi.org/10.1080/00207543.2021.1897178.
Zhang, Z., Li, L., Cai, N., Jia, L., 2019. Local neighborhood genetic algorithm for stochastic disassembly line balancing problem. Comput. Integr. Manuf. Syst. 25 (3), 607–618. https://doi.org/10.13196/j.cims.2019.03.008.
Zhang, Z., Wang, K., Zhu, L., Cheng, W., 2018. Pareto hybrid ant colony and genetic algorithm for multi-objective U-shaped disassembly line balancing problem. J. Southwest Jiaot. Univ. 53 (3), 628–660. https://doi.org/10.3969/j.issn.0258-2724.2018.03.026.
Zhang, Z., Wang, K., Zhu, L., Wang, Y., 2017. A Pareto improved artificial fish swarm algorithm for solving a multi-objective fuzzy disassembly line balancing problem. Expert Syst. Appl. 86, 165–176. https://doi.org/10.1016/j.eswa.2017.05.053.
Zhu, L.X., Zhang, Z.Q., Guan, C., 2020. Multi-objective partial parallel disassembly line balancing problem using hybrid group neighbourhood search algorithm. J. Manuf. Syst. 56, 252–269. https://doi.org/10.1016/j.jmsy.2020.06.013.
Zhu, L., Zhang, Z., Wang, Y., 2018. A Pareto firefly algorithm for multi-objective disassembly line balancing problems with hazard evaluation. Int. J. Prod. Res. 56 (24), 7354–7374. https://doi.org/10.1080/00207543.2018.1471238.
Zhu, L., Zhang, Z., Wang, Y., Cai, N., 2020. On the end-of-life state oriented multi-objective disassembly line balancing problem. J. Intell. Manuf. 31 (6), 1403–1428. https://doi.org/10.1007/s10845-019-01519-3.
Zou, B., Zhang, Zeqiang, Cai, N., Zhu, L., 2018. Cat swarm simulated annealing algorithm for disassembly line balancing problem under tool constraints. Comput. Integr. Manuf. Syst. 24 (9), 2210–2222. https://doi.org/10.13196/j.cims.2018.09.009.